



ANALYSIS OF THICK LAMINATED ANISOTROPIC CYLINDRICAL SHELLS USING A REFINED SHELL THEORY

HUNG-SYING JING and KUANG-GOANG TZENG

Institute of Aeronautics and Astronautics, National Cheng Kung University, Tainan,
 Taiwan 70101, People's Republic of China

(Received 9 June 1993; in revised form 23 June 1994)

Abstract—Bending analysis of arbitrarily laminated, anisotropic panels and closed cylinders using the mixed shear deformation theory proposed by the authors is presented. A set of equilibrium, transverse shear compatibility and boundary conditions are obtained by using the mixed variational principle proposed by Jing and Liao (1989, *Int. J. Numer. Meth. Engng* **28**, 2813–2827) with displacements and transverse shear as independent variables. The zig-zag type displacement is assumed together with piecewise parabolic transverse shear. The initial curvature effect is included in the strain–displacement relations, stress resultants and assumed transverse shear stresses. Two types of shell geometry, infinitely long cylindrical panels and closed cylinders of finite length, are employed in the numerical study. The cylindrical panels considered are subjected to a transversely sinusoidal loading, while closed cylinders are under an uniform internal pressure. Numerical results presented here are compared with exact three-dimensional elasticity solutions. From these comparisons, it is found that this mixed shear deformation theory can supply reasonably good results.

NOMENCLATURE

A_1, A_2	coefficients of the first quadratic form of the middle surface
C_{ij}	elastic moduli
E_L, E_T	Young's moduli
G_{LT}, G_{TT}	shear moduli
h	total thickness of the shell
h_k	thickness of the k th layer
k_1, k_2	principle curvatures of the middle surfaces
$K_{xz}, K_{\theta z}$	transverse shear stress resultants corresponding to zig-zag components
L	length of the shell
$L_{\alpha\beta}$	in-plane stress resultants corresponding to zig-zag components
$M_{\alpha\beta}: M_x, M_{x\theta}, M_{\theta x}, M_\theta$	moment stress resultants
N	number of layers in the shell
$N_{\alpha\beta}: N_x, N_{x\theta}, N_{\theta x}, N_\theta$	in-plane stress resultants
$N_{xz}, N_{\theta z}$	transverse shear stress resultants
$Q_x^{(k)}$	the parabolic part of shear force in the x direction
R	mean radius of cylindrical shell
$R^{(k)}$	mean radius of the k th layer
S_{xx}, S_θ	amplitudes of zig-zag in-plane displacements
S_{44}, S_{45}, S_{55}	compliances for transverse shear
T_z^+, T_z^-	prescribed tractions on the top and bottom surfaces
$T_x^{(k)}$	the values of transverse shear in the x direction at the k th interface
U_x, U_θ, U_z	displacements of the middle surface in the x, θ and z coordinates
Ψ_x, Ψ_θ	rotations of the middle surface
v_x, v_θ	direction cosines of unit normal
ν_{LT}, ν_{TT}	Poisson's ratio
ϕ	the open angle of the panel

INTRODUCTION

A shell is a curved structure and has many applications. The presence of curvature effectively increases the structural stiffness. On the other hand, as everyone knows, fiber reinforced composite materials provide certain advantages such as low weight to stiffness and weight to strength ratios, good corrosion and heat resistance, and improved fatigue life. As a result, shells made of composites are extensively used in aircraft structures, pressure vessels, sporting equipment, automobiles, and so on. Among the various constructions of shells,

the closed cylindrical shells, panels and doubly curved shells are very important. Therefore, bending analysis of these structures has received wide attention in recent years.

Based on the classical lamination theory incorporating the Kirchhoff–Love hypotheses, also known as the Love first approximation theory, the static analysis of laminated shells has been studied by Whitney and Halpin (1968), Whitney (1971), Reuter (1972), Chaudhuri *et al.* (1986) and Simites and Han (1991). These theories are adequate to predict the global response of laminates with relatively small thickness. Because of the low shear modulus to in-plane stiffness ratio, the important role of transverse shear deformation, which is not contained in classical lamination theory, cannot be neglected. Consequently, first-order or high-order shear deformation theories of fiber reinforced laminated shells for more accurate stresses and deformations were proposed by Dong and Tso (1972), Reddy (1984), Reddy and Liu (1985), Chaudhuri and Abu-Arja (1989), Khdeir *et al.* (1989) and Dennis and Palazotto (1991).

All the previously mentioned theories classified as the displacement based theories will in general violate the condition of traction continuity at layer interface unless employing the very specially designed displacement field by Hsu and Wang (1970) and Di Sciuva (1987). To overcome this drawback, Reissner (1987) proposed another type of general shell theory for transversely isotropic materials based on the Reissner mixed variational principle (Reissner, 1984) with independently assumed transverse stresses. Recently, Jing and Liao (1989) proposed a mixed functional with displacements and transverse shear stresses as independent variables and established the corresponding partial hybrid stress element for the analysis of thick laminated plates. Some comparisons between these two functionals for plates are made by Jing and Tzeng (1993a). More recently, Jing and Tzeng (1993b) derived a mixed shear deformation theory for thick laminated shells of general shape based on the functional proposed by Jing and Liao (1989). In this theory, the zig-zag type of displacement field is assumed in addition to the Mindlin displacement by Murakami (1986). There are seven independent displacement variables in total, three displacements for the middle surface, two slopes and two zig-zag type displacements through the thickness. Piecewise parabolic transverse shear stresses satisfying interface continuity are assumed independently and the initial curvature effect is also included. In the previous study, the cross-ply shells are used and satisfactory results are obtained by Jing and Tzeng (1993b).

The purpose of the present study is to further investigate the range of application of this mixed shear deformation theory (Jing and Tzeng, 1993b) for generally laminated anisotropic shells. Two types of shell geometry, cylindrical panels and closed finite circular cylinders are considered. The panels are subjected to a transverse sinusoidal loading, while the closed cylinders are under a uniform internal pressure. Numerical results are compared with exact three-dimensional elasticity solutions, obtained by Jing and Tzeng (1993c,d), and some discussions are made.

GOVERNING EQUATIONS

For the sake of brevity, the equations of motion derived for general shells (Jing and Tzeng, 1993b) are not restated here. For a particular type of shell the governing equations can be easily obtained by substituting the first fundamental form and curvatures. For cylindrical shells, they become

$$A_1 = 1; \quad A_2 = R; \quad k_1 = 0; \quad k_2 = \frac{1}{R} \quad (1)$$

where R is mean radius of the cylinder. The $A_x = A_x(\xi_1, \xi_2)$ are coefficients of the first quadratic form of the middle surface, and $k_x = k_x(\xi_1, \xi_2)$ are principal curvatures of the middle surface along the lines $\xi_2 = \text{constant}$, $\xi_1 = \text{constant}$, respectively. The x, θ and z represent the axial, circumferential and thickness coordinates. Static equilibrium equations for cylindrical shells subjected to transverse normal loading can thus be obtained as

$$\begin{aligned}
 N_{x,x} + \frac{1}{R}N_{x\theta,\theta} &= 0; & N_{\theta x,x} + \frac{1}{R}(N_{\theta,\theta} + N_{\theta z}) &= 0 \\
 N_{xz,x} + \frac{1}{R}N_{\theta z,\theta} - \frac{1}{R}N_{\theta} + (T_z^+ - T_z^-) + \frac{h}{2R}(T_z^+ + T_z^-) &= 0 \\
 M_{x,x} + \frac{1}{R}M_{\theta x,x} - N_{xz} &= 0; & M_{x\theta,x} + \frac{1}{R}M_{\theta,\theta} - N_{\theta z} &= 0 \\
 L_{x,x} + \frac{1}{R}L_{\theta x,x} - K_{xz} &= 0; & L_{x\theta,x} + \frac{1}{R}L_{\theta,\theta} - K_{\theta z} &= 0.
 \end{aligned} \tag{2}$$

T_z^+, T_z^- stand for the normal tractions on the top and bottom surfaces and h the total thickness. The stress resultants can also be found in previous work (Jing and Tzeng 1993b). There are seven equations in total regardless of the number of layers. It should be noted that the initial curvature effect is included in the stress resultants. This results in the nonsymmetric stress resultants, i.e. $N_{x\theta} \neq N_{\theta x}$, $M_{x\theta} \neq M_{\theta x}$, and $L_{x\theta} \neq L_{\theta x}$.

Using the same assumed transverse shear stresses (Jing and Tzeng 1993b), piecewise parabolic and the functional proposed by Jing and Liao (1989), the transverse shear compatibility equations of arbitrarily laminated anisotropic cylindrical shells can be expressed in matrix form as follows:

$$\begin{aligned}
 \mathbf{Q}_x + \mathbf{A}_1 \mathbf{T}_x + \mathbf{B}_1 \mathbf{Q}_\theta + \mathbf{A}_2 \mathbf{T}_\theta &= \mathbf{d}_1 \gamma_{xz}^0 + \mathbf{d}_2 S_x \\
 \mathbf{F}_1 \mathbf{Q}_x + \mathbf{F}_2 \mathbf{Q}_\theta + \mathbf{G}_1 \mathbf{T}_x + \mathbf{G}_2 \mathbf{T}_\theta &= \mathbf{d}_3 \gamma_{xz}^0 + \mathbf{d}_4 S_x \\
 \mathbf{B}_2 \mathbf{Q}_x + \mathbf{Q}_\theta + \mathbf{A}_3 \mathbf{T}_x + \mathbf{A}_4 \mathbf{T}_\theta &= \mathbf{d}_5 \gamma_{\theta z}^0 + \mathbf{d}_6 S_\theta \\
 \mathbf{F}_3 \mathbf{Q}_x + \mathbf{F}_4 \mathbf{Q}_\theta + \mathbf{G}_2 \mathbf{T}_x + \mathbf{G}_3 \mathbf{T}_\theta &= \mathbf{d}_7 \gamma_{\theta z}^0 + \mathbf{d}_8 S_\theta.
 \end{aligned} \tag{3}$$

In the above formula

$$\begin{aligned}
 \mathbf{Q}_\alpha &= [Q_\alpha^{(1)} \quad Q_\alpha^{(2)} \quad \dots \quad Q_\alpha^{(N)}]^\top \\
 \mathbf{T}_\alpha &= [T_\alpha^{(1)} \quad T_\alpha^{(2)} \quad \dots \quad T_\alpha^{(N-1)}]^\top
 \end{aligned}$$

where $\alpha = 1, 2$ representing x and θ . The $Q_\alpha^{(k)}$ represents the parabolic part of shear force in the α direction of the k th layer. $T_\alpha^{(k)}$ is the value of the transverse shear at the k th interface along the α direction. The matrices $\mathbf{d}_i (i = 1-8)$, \mathbf{A}_j , $\mathbf{F}_j (j = 1-4)$, $\mathbf{G}_i (i = 1-3)$ and $\mathbf{B}_\beta (\beta = 1, 2)$ are expressed in eqn (A1) in the Appendix. The boundary conditions are given by

Geometric (essential)	Force (natural)
$U_x = 0$	$N_x v_x + N_{\theta x} v_\theta = 0$
$U_\theta = 0$	$N_{x\theta} v_x + N_\theta v_\theta = 0$
$U_z = 0$	$N_{xz} v_x + N_{\theta z} v_\theta = 0$
$\Psi_x = 0$	$M_x v_x + M_{\theta x} v_\theta = 0$
$\Psi_\theta = 0$	$M_{x\theta} v_x + M_\theta v_\theta = 0$
$S_x = 0$	$L_x v_x + L_{\theta x} v_\theta = 0$
$S_\theta = 0$	$L_{x\theta} v_x + L_\theta v_\theta = 0$

where (v_x, v_θ) are direction cosines of unit normal to the boundary of the middle surface. If the boundary is simply supported, it means $U_z = M_\theta = N_\theta = L_\theta = 0$ along the x direction, and $U_z = M_x = N_x = L_x = 0$ along the θ direction.

The constitutive equations of in-plane stress resultants, which can be derived directly from the Hooke law of the material, strain–displacement relations, and the stress resultants, for the laminated anisotropic cylindrical shells and panels are of the form

$$\begin{Bmatrix} \mathbf{N} \\ \mathbf{M} \\ \mathbf{L} \end{Bmatrix} = \begin{bmatrix} \mathbf{N}_\epsilon & \mathbf{N}_\kappa & \mathbf{N}_\beta \\ \mathbf{N}_\kappa & \mathbf{M}_\kappa & \mathbf{M}_\beta \\ \mathbf{N}_\beta & \mathbf{M}_\beta & \mathbf{L}_\beta \end{bmatrix} \begin{Bmatrix} \mathbf{U}_\epsilon \\ \mathbf{U}_\kappa \\ \mathbf{U}_\beta \end{Bmatrix} \tag{5}$$

where

$$\begin{aligned} \mathbf{N} &= [N_x N_\theta N_{x\theta} N_{\theta x}]^T & \mathbf{M} &= [M_x M_\theta M_{x\theta} M_{\theta x}]^T \\ \mathbf{L} &= [L_x L_\theta L_{x\theta} L_{\theta x}]^T & \mathbf{U}_\epsilon &= [\epsilon_x^0 \epsilon_\theta^0 \epsilon_{x\theta}^0 \epsilon_{\theta x}^0]^T \\ \mathbf{U}_\kappa &= [\kappa_x \kappa_\theta \kappa_{x\theta} \kappa_{\theta x}]^T & \mathbf{U}_\beta &= [\beta_x \beta_\theta \beta_{x\theta} \beta_{\theta x}]^T \\ \mathbf{N}_\epsilon &= \begin{bmatrix} H_{11} & A_{12} & H_{16} & A_{16} \\ A_{12} & G_{22} & A_{26} & G_{26} \\ H_{16} & A_{26} & H_{66} & A_{66} \\ A_{16} & G_{26} & A_{66} & G_{66} \end{bmatrix} & \mathbf{N}_\kappa &= \begin{bmatrix} T_{11} & B_{12} & T_{16} & B_{16} \\ B_{12} & F_{22} & B_{26} & F_{26} \\ T_{16} & B_{26} & T_{66} & B_{66} \\ B_{16} & F_{26} & B_{66} & F_{66} \end{bmatrix} \\ \mathbf{N}_\beta &= \begin{bmatrix} R_{11} & 0 & R_{16} & 0 \\ 0 & E_{22} & 0 & E_{26} \\ R_{16} & 0 & R_{66} & 0 \\ 0 & E_{26} & 0 & E_{66} \end{bmatrix} & \mathbf{M}_\kappa &= \begin{bmatrix} I_{11} & D_{12} & I_{16} & D_{16} \\ D_{12} & P_{22} & D_{26} & P_{26} \\ I_{16} & D_{26} & I_{66} & D_{66} \\ D_{16} & P_{26} & D_{66} & P_{66} \end{bmatrix} \\ \mathbf{M}_\beta &= \begin{bmatrix} J_{11} & K_{12} & J_{16} & K_{16} \\ K_{12} & Q_{22} & K_{26} & Q_{26} \\ J_{16} & K_{26} & J_{66} & K_{66} \\ K_{16} & Q_{26} & K_{66} & Q_{66} \end{bmatrix} & \mathbf{L}_\beta &= \begin{bmatrix} X_{11} & Y_{12} & X_{16} & Y_{16} \\ Y_{12} & Z_{22} & Y_{26} & Z_{26} \\ X_{16} & Y_{26} & X_{66} & Y_{66} \\ Y_{16} & Z_{26} & Y_{66} & Z_{66} \end{bmatrix} \end{aligned}$$

The elements of the above matrices are defined as

$$(A_{ij}, B_{ij}, D_{ij}, K_{ij}, Y_{ij}) = \sum_{k=1}^N \int_{\Omega^{(k)}} C_{ij}^{(k)} \left(1, z, z^2, (-1)^k \frac{2}{h_k} z z^{(k)}, \frac{4}{h_k^2} z^{(k)^2} \right) dz \tag{6a}$$

$$\begin{aligned} (H_{ij}, R_{ij}, T_{ij}, I_{ij}, J_{ij}, X_{ij}) &= \sum_{k=1}^N \int_{\Omega^{(k)}} C_{ij}^{(k)} \left(1 + \frac{z}{R} \right) \left(1, z, \right. \\ &\quad \left. (-1)^k \frac{2}{h_k} z^{(k)}, z^2, (-1)^k \frac{2}{h_k} z z^{(k)}, \frac{4}{h_k^2} z^{(k)^2} \right) dz \end{aligned} \tag{6b}$$

$$\begin{aligned} (G_{ij}, F_{ij}, E_{ij}, P_{ij}, Q_{ij}, Z_{ij}) &= \sum_{k=1}^N \int_{\Omega^{(k)}} C_{ij}^{(k)} \frac{1}{1 + \frac{z}{R}} \left(1, z, \right. \\ &\quad \left. (-1)^k \frac{2}{h_k} z^{(k)}, z^2, (-1)^k \frac{2}{h_k} z z^{(k)}, \frac{4}{h_k^2} z^{(k)^2} \right) dz \end{aligned} \tag{6c}$$

for $i, j = 1, 2, 6$ in this case. The strain components are

$$\begin{aligned}
 \varepsilon_x^0 &= U_{x,x}; & \varepsilon_\theta^0 &= \frac{1}{R}(U_z + U_{\theta,\theta}); & \varepsilon_{x\theta}^0 &= U_{\theta,x} \\
 \varepsilon_{\theta x}^0 &= \frac{1}{R}U_{x,\theta}; & \kappa_x &= \Psi_{x,x}; & \kappa_\theta &= \frac{1}{R}\Psi_{\theta,\theta} \\
 \kappa_{x\theta} &= \Psi_{\theta,x}; & \kappa_{\theta x} &= \frac{1}{R}\Psi_{x,\theta}; & \beta_x &= S_{x,x} \\
 \beta_\theta &= \frac{1}{R}S_{\theta,\theta}; & \beta_{x\theta} &= S_{\theta,x}; & \beta_{\theta x} &= \frac{1}{R}S_{x,\theta}.
 \end{aligned} \tag{7}$$

In the above formula, U_x , U_θ , and U_z stand for the displacements of the middle surface in the x , θ and z directions. Ψ_x and Ψ_θ are rotations of the middle surface about the θ and x directions. S_x and S_θ are the amplitudes of the zig-zag in-plane displacement variations across the thickness of the shell. The transverse shear resultants can be obtained through the assumed transverse shear stresses. The results are

$$\begin{Bmatrix} N_{xz} \\ N_{\theta z} \\ K_{xz} \\ K_{\theta z} \end{Bmatrix} = \begin{bmatrix} D_{11}^* & D_{12}^* & D_{13}^* & D_{14}^* \\ G_{11}^* & G_{12}^* & G_{13}^* & G_{14}^* \\ D_{21}^* & D_{22}^* & D_{23}^* & D_{24}^* \\ G_{21}^* & G_{22}^* & G_{23}^* & G_{24}^* \end{bmatrix} \begin{Bmatrix} \gamma_{xz}^0 \\ S_x \\ \gamma_{\theta z}^0 \\ S_\theta \end{Bmatrix} \tag{8}$$

where $\gamma_{xz}^0 = U_{z,x} + \Psi_x$ and $\gamma_{\theta z}^0 = (1/R)(U_{z,\theta} - U_\theta) + \Psi_\theta$, and $D_{11}^*, \dots, G_{24}^*$ are given in eqn (A2) in the Appendix. Substituting eqns (5) and (8) into eqn (2), the final equilibrium equation is then in terms of displacement variables and ready to be solved with appropriate methods. In this paper, series method is used to find the solution. For an infinitely long shell in the x direction, the governing equations can be obtained by neglecting quantities involving the derivatives of x . Similarly, the governing equations for an axisymmetric problem is then obtained by neglecting quantities involving the derivatives of θ .

NUMERICAL EXAMPLES

In order to verify the accuracy of the present mixed shear deformation theory for generally anisotropic shells, two numerical examples are considered. One consists of cylindrical shell panels of infinite length in the axial direction under transverse normal loading, the other is a closed cylinder of finite length subjected to a uniform internal pressure in which the problem is independent of θ coordinates. The corresponding geometries and coordinate systems are given in Figs 1(a) and (b) separately. The solutions obtained from the present theory for these examples are compared with exact solutions obtained by Jing and Tzeng (1993c, d).

Example 1: cylindrical panels

In the first example, a cylindrical panel with mean radius R and thickness h is subjected to a sinusoidal loading [$T_z^+ = q_0 \sin(\pi\theta/\phi)$] with maximum value q_0 at the center. The boundary is simply supported. The open angle of the panel is denoted by ϕ and the angle θ used in the following discussion is defined as $0 \leq \theta \leq \phi$. Two types of stacking sequences, a two-layered antisymmetric [$45^\circ/-45^\circ$] laminate and a three-layered symmetric [$45^\circ/-45^\circ/46^\circ$] laminate are considered. The layers are of equal thickness. The negative sign of the fiber angle denotes counterclockwise direction with respect to the positive direction of the generator (x axis). For ease of comparison, the following material properties, geometry and normalized parameters are considered:

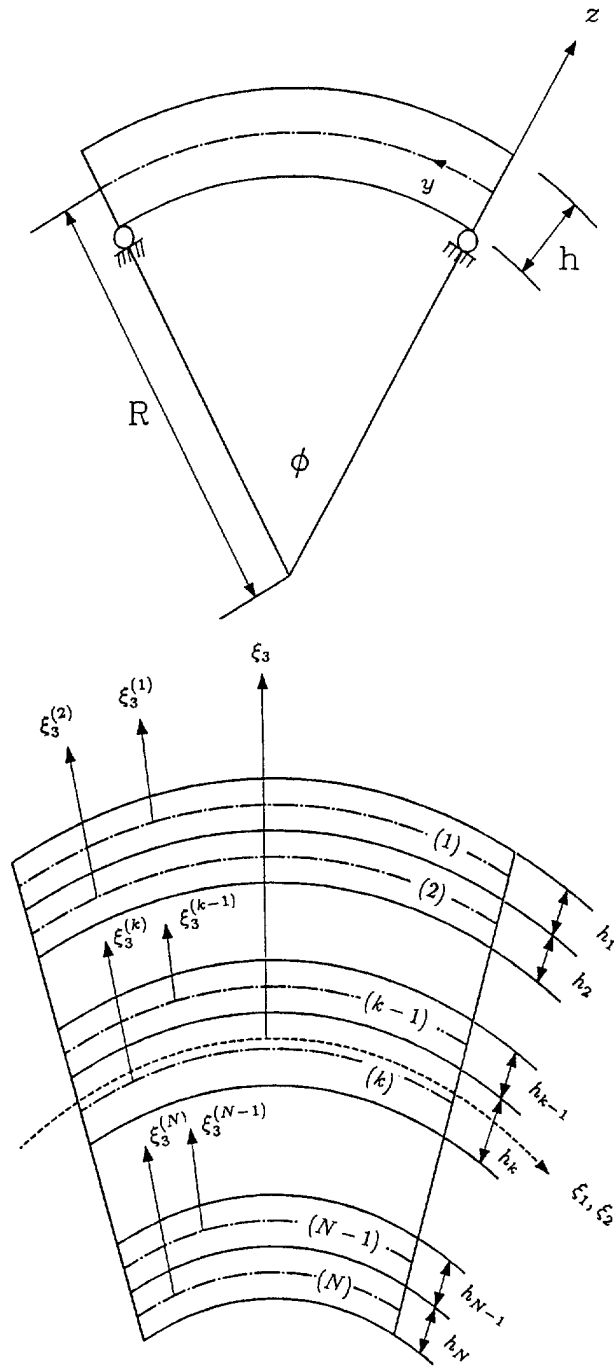


Fig. 1(a). Cylindrical panel coordinates and geometry; (b) shell coordinates, geometry and lamination.

$$E_L/E_T = 40; \quad G_{LT}/E_T = 0.5; \quad G_{TT}/E_T = 0.2$$

$$v_{LT} = 0.25; \quad v_{TT} = 0.25; \quad S = \frac{R}{h}; \quad \phi = \frac{\pi}{3}; \quad \bar{z} = \frac{z}{h}$$

$$(\bar{u}_z, \bar{u}_\theta) = \frac{E_T}{q_0 h} \left(\frac{100u_z}{S^4}, \frac{u_\theta}{S^3} \right)$$

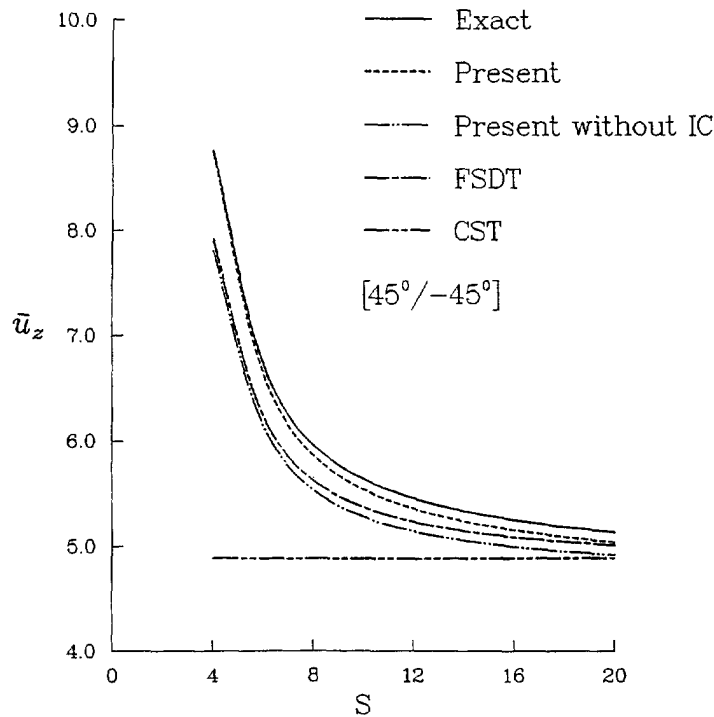


Fig. 2. Comparisons of central transverse deflection $\bar{u}_z(\phi/2, z)$ of $[45^\circ/-45^\circ]$ laminate from elasticity, present, FSDT and CST with various S values.

$$(\bar{\sigma}_z, \bar{\sigma}_\theta, \bar{\sigma}_x, \bar{\tau}_{\theta z}) = \frac{1}{q_0} \left(\sigma_z, \frac{\sigma_\theta}{S^2}, \frac{\sigma_x}{S^2}, \frac{\tau_{\theta z}}{S} \right) \quad (9)$$

where L denotes the direction parallel to the fibers, T the transverse direction, and ν the Poisson ratio. Moreover, u_x , u_θ and u_z denote the displacements along axial, circumferential and thickness directions.

Figures 2 and 3 show the influence of radius to thickness ratio (S) on the central transverse deflection \bar{u}_z for both stacking sequences. Three approaches, namely the classical shell theory (CST), first-order shear deformation theory (FSDT) (Reddy, 1984) and the present one, are compared with the exact theory by Jing and Tzeng (1993c). In these figures, the ratio S ranges from 4 to 20. For both stacking sequences, the present results are all very close to that from the elasticity solution. As S increases, the results of these three theories are asymptotically close to the exact theory. Moreover, it is seen that the present results for symmetric configuration are more accurate than antisymmetric layup as S increases. These figures also show the influence of the initial curvature (IC) effect on the transverse deflection with various S for both stacking sequences. The deviations caused by neglecting the IC are very clear. The errors of \bar{u}_z without considering IC for $S = 4, 20$ are 10.9% and 4.2% while they are 0.4% and 1.8% for the results with IC. Therefore, the incorporation of IC in the two-dimensional shell theory for accurate results is a must.

Figures 4 and 5 display the comparisons of the circumferential displacements at the edge point $\theta = 0$ for both stacking sequences from CST, the present approach and the exact theory. In these figures, a shell panel with $S = 4$ is used. These figures show that the present results are very close to the elasticity solution. For $[45^\circ/-45^\circ]$ layup, the zig-zag amplitudes S_x and S_θ are almost zero which results in the through thickness distributions of circumferential displacement \bar{u}_θ very close to linear. On the other hand, the zig-zag shape is more obvious for $[45^\circ/-45^\circ/45^\circ]$ lamination.

Through thickness stresses $\bar{\sigma}_\theta$ along the circumferential direction at the point $\theta = \phi/2$, from three different theories with $S = 4$, are plotted in Figs 6 and 7 for both stacking sequences. Again, it can be found that the present results are in good agreement with the

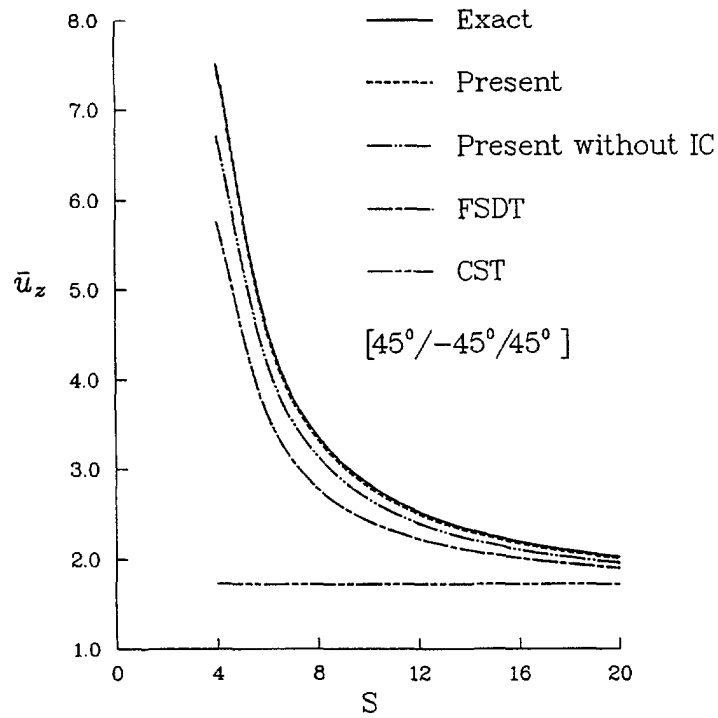


Fig. 3. Comparisons of central transverse deflection $\bar{u}_z(\phi/2, z)$ of $[45^\circ/-45^\circ/45^\circ]$ laminate from elasticity, present, FSDT and CST with various S values.

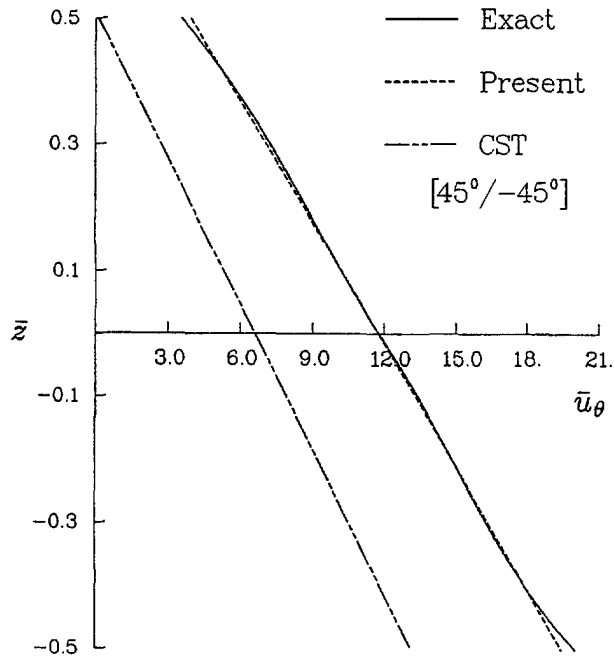


Fig. 4. Comparisons of the through thickness circumferential displacement $\bar{u}_\theta(0, z)$ of $[45^\circ/-45^\circ]$ laminate from elasticity, present and CST with $S = 4$.

elasticity solution. Obviously, the results from CST for $[45^\circ/-45^\circ]$ layup are more accurate than $[45^\circ/-45^\circ/45^\circ]$ lamination. The reason is thought to be as follows. Although the deviations of displacements are significantly large for both stacking sequences, the derivatives of them are fairly close to the exact theory for $[45^\circ/-45^\circ]$ layup.

Figures 8 and 9 exhibit the through thickness distributions of transverse shear stress $\bar{\tau}_{\theta z}$ at the point $\theta = 0$ for $S = 4$. Since the traction free conditions on the top and bottom

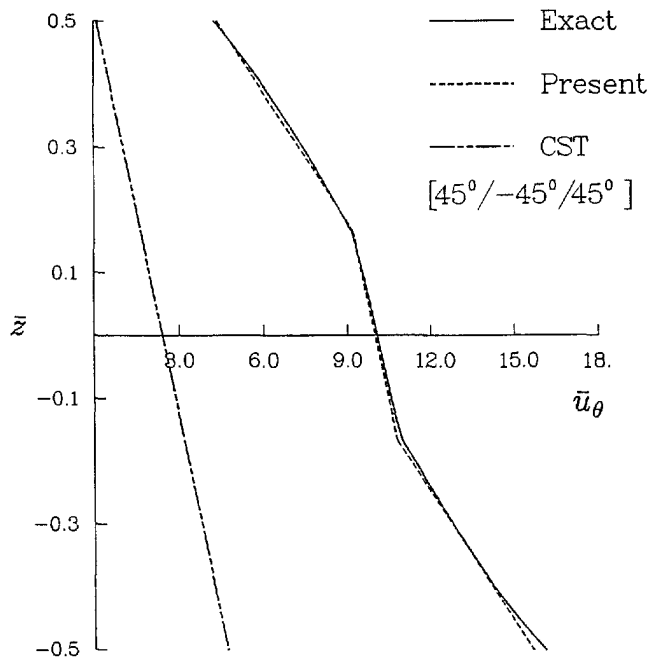


Fig. 5. Comparisons of the through thickness circumferential displacement $\bar{u}_\theta(0, z)$ of $[45^\circ/-45^\circ/45^\circ]$ laminate from elasticity, present and CST with $S = 4$.

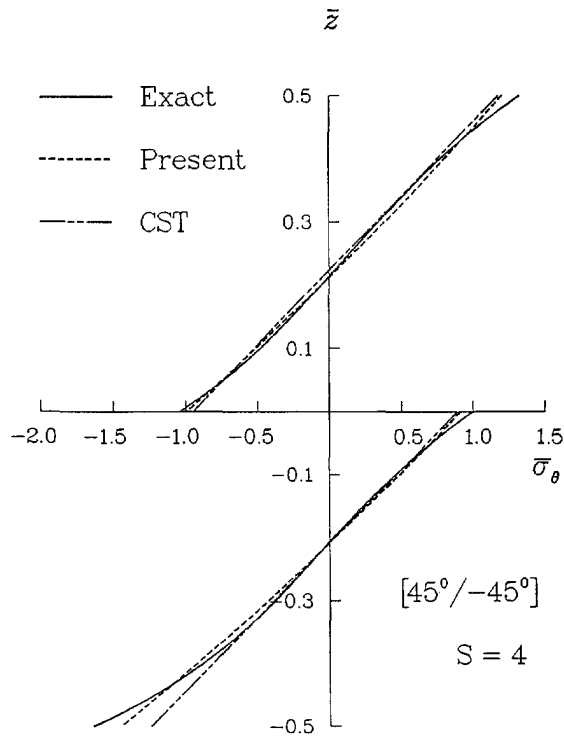


Fig. 6. Comparisons of the through thickness circumferential stress $\bar{\sigma}_\theta(\phi/2, z)$ of $[45^\circ/-45^\circ]$ laminate elasticity, present and CST with $S = 4$.

surfaces and the continuity conditions along interfaces are satisfied in the assumed transverse shear fields, unreasonable discontinuity phenomena do not show up in the present approach. As compared with the elasticity solution, the present results are fairly accurate. Further, the present approach with IC, which makes the distribution nonsymmetric, on assumed transverse shear stresses has the same tendency as the exact theory. However,

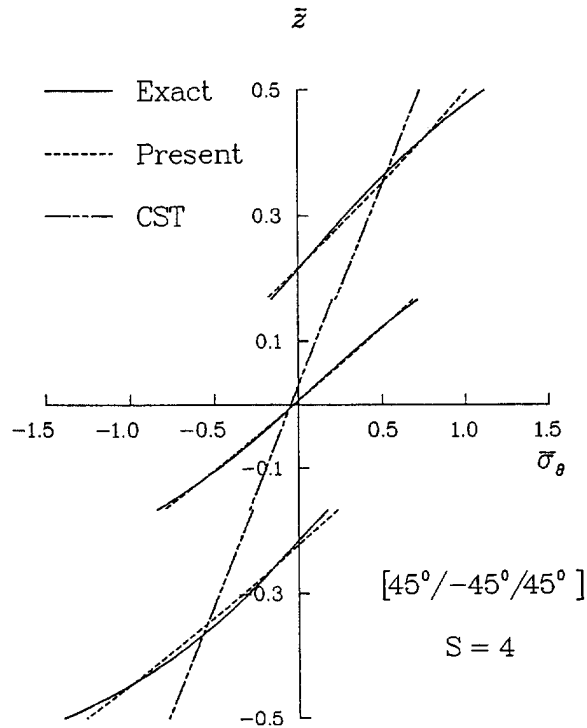


Fig. 7. Comparisons of the through thickness circumferential stress $\bar{\sigma}_\theta(\phi/2, z)$ of $[45^\circ/-45^\circ/45^\circ]$ laminate from elasticity, present and CST with $S = 4$.

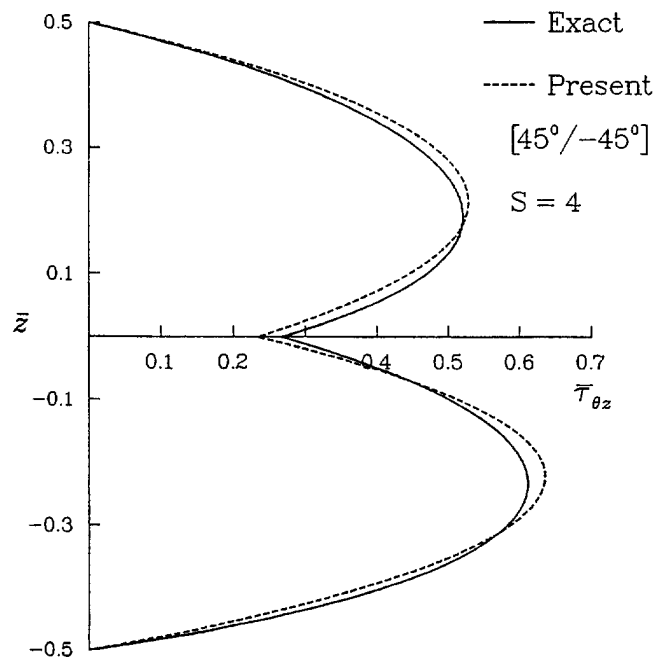


Fig. 8. Comparisons of the through thickness transverse shear stress $\bar{\tau}_{\theta z}(0, z)$ of $[45^\circ/-45^\circ]$ laminate from elasticity and present with $S = 4$.

discrepancies can still be found along the ply interfaces. In composite laminated shells, the transverse normal stress is very important because it is related to the delamination. The transverse normal stresses of this example are plotted in Figs 10 and 11. Since the transverse and in-plane displacements assumed in this theory are of zero and first order, respectively, the corresponding stress will not be reasonable if it is obtained directly from the stress-

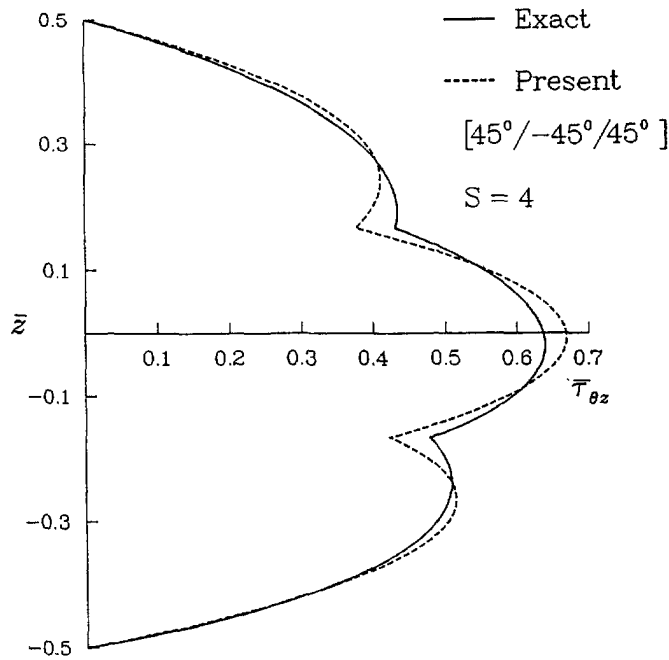


Fig. 9. Comparisons of the through thickness circumferential shear stress $\bar{\tau}_{\theta z}(0, z)$ of $[45^\circ/-45^\circ/45^\circ]$ laminate from elasticity and present with $S = 4$.

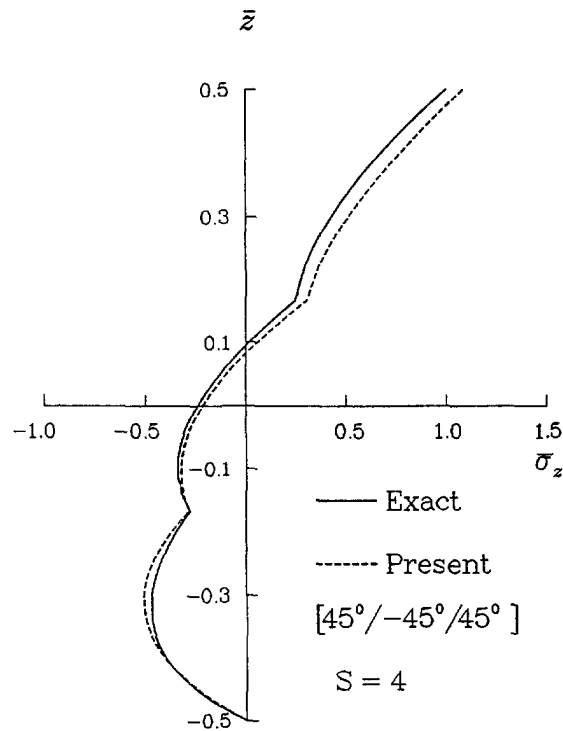


Fig. 10. Comparisons of the through thickness normal stress $\bar{\sigma}_z(\phi/2, z)$ of $[45^\circ/-45^\circ]$ laminate from elasticity and present with $S = 4$.

strain relation. Consequently, the exact equilibrium equation in the transverse direction is integrated to obtain the transverse normal stress by using the transverse shear obtained in Figs 8 and 9. From the comparisons, it can be seen that the results from this theory are fairly acceptable. In symmetric layup, the comparison is even better.

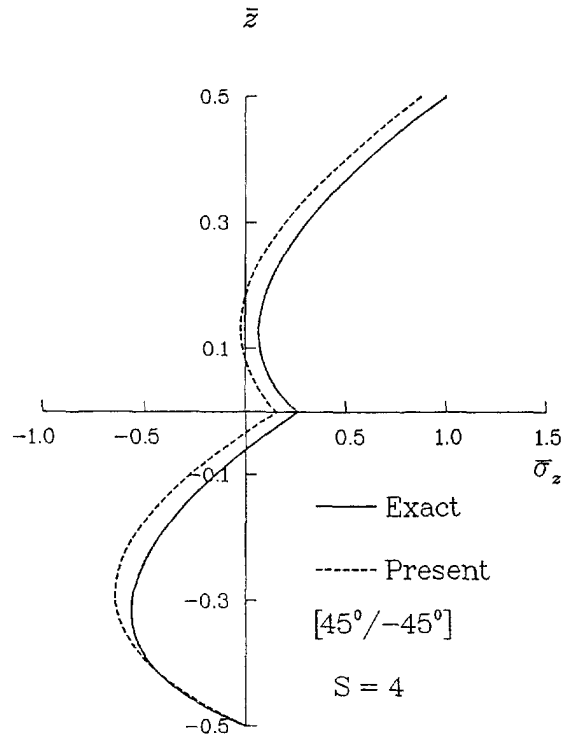


Fig. 11. Comparisons of the through thickness transverse normal stress $\bar{\sigma}_z(\phi/2, z)$ of $[45^\circ/-45^\circ/45^\circ]$ laminate from elasticity and present with $S = 4$.

Example 2: finite cylinders

In the second example, a three-layered symmetric closed finite cylinder with stacking sequence $[-45^\circ/45^\circ/-45^\circ]$ is considered. The layers are of equal thickness. A uniform internal pressure with intensity p_0 is applied on the inner surface. The boundary is again simply supported. Material properties and non-dimensionalized displacements and stresses are considered :

$$E_L/E_T = 40; \quad G_{LT}/E_T = 0.5; \quad G_{TT}/E_T = 0.2 \tag{10}$$

$$v_{LT} = 0.25; \quad v_{TT} = 0.49; \quad S = \frac{R}{h}; \quad \frac{L}{R} = 20 \tag{11}$$

$$\bar{u}_z = \frac{10E_T h}{p_0 R^2} u_z; \quad (\bar{\sigma}_x, \bar{\sigma}_\theta, \bar{\tau}_{xz}, \bar{\tau}_{x\theta}) = \frac{1}{p_0} (\sigma_x, \sigma_\theta, \tau_{xz}, \tau_{x\theta}). \tag{12}$$

In the above formulae, R, h, L denote the mean radius, thickness and length of the cylinder. Figures 12–16 display results of the second example. In these figures a closed cylinder with $S = 5$ is investigated. Figure 12 shows the comparisons of transverse deflection between CST, the present approach and the exact theory (approximate elasticity solution) obtained by Jing and Tzeng (1993d). It is seen that the deflections are all very uniform in the central region, but some variations can be found in the edge region. Since the applied load is on the bottom surface, while CST on the middle surface, the results from CST have certain deviations, up to 13% in the central region. From this comparison, the present approach gives results almost identical to that of exact theory in the central region. There is only a minor deviation at the edge. The main reason for this good comparison both in the central and edge regions is because the present approach includes the effect of initial curvature and shear deformation, which is considered by using a mixed formulation.

Axial variations of in-plane stresses at the top surface of the outer layer are shown in Figs 13–15. In these figures, the results from CST, approximate elasticity, and the present

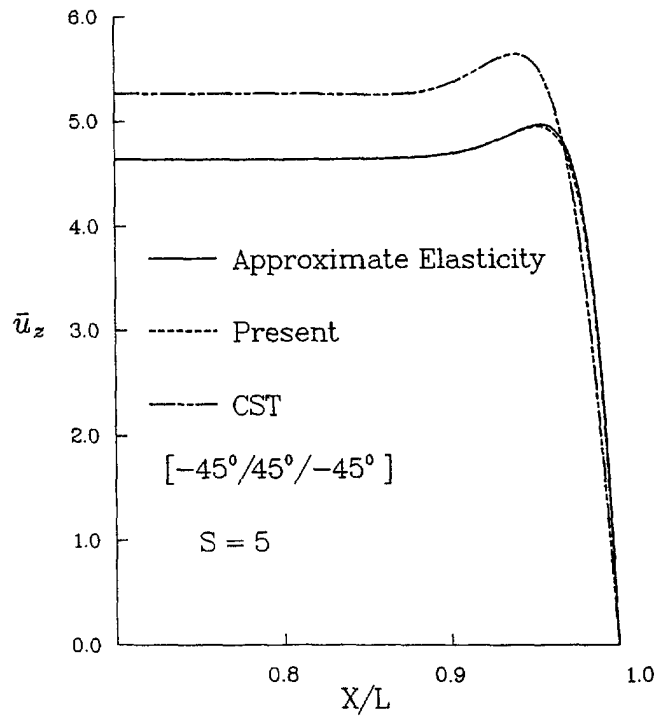


Fig. 12. Comparisons of axial variation of transverse deflection of the middle surface of $[-45^\circ/45^\circ/45^\circ]$ laminate from elasticity, present and CST with $S = 5$.

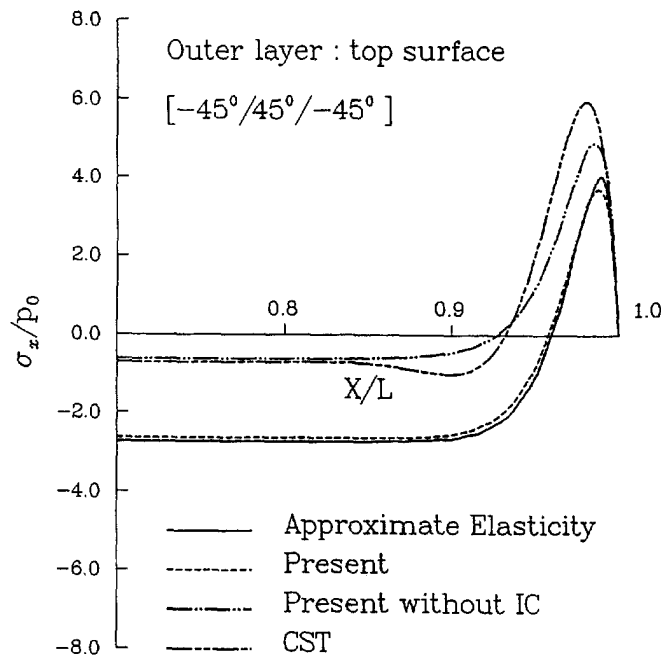


Fig. 13. Comparisons of axial variation of longitudinal stress of the top surface of $[-45^\circ/45^\circ/45^\circ]$ laminate from elasticity, present and CST with $S = 5$.

approach are given. The solution of the present theory without the initial curvature effect is also included to reveal the importance of this effect. For all the in-plane stresses, the axial stress $\bar{\sigma}_x$, circumferential stress $\bar{\sigma}_\theta$ and shear stress $\bar{\tau}_{x\theta}$, the present approach gives reasonably good agreement both in the central and edge regions when compared with the elasticity solution. The results from CST show great deviation throughout the length of the shell. If the effect of shear deformation is included, the results in the edge region are closer to that

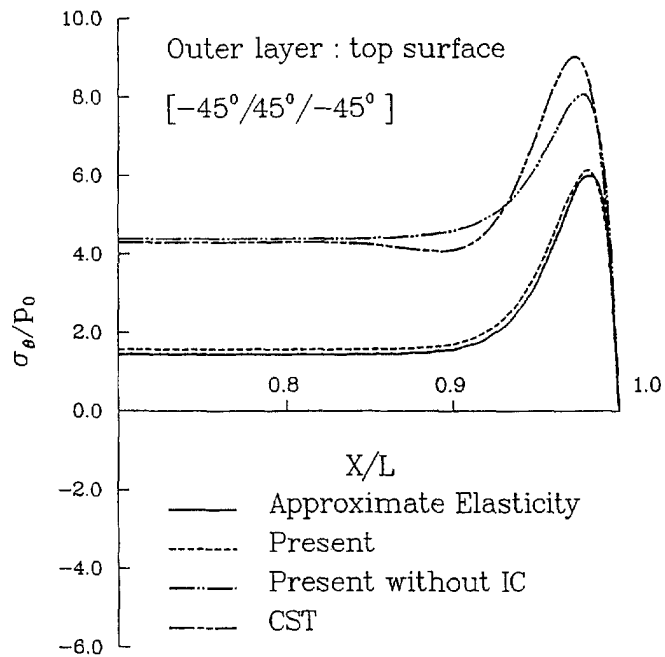


Fig. 14. Comparisons of axial variation of circumferential stress of the top surface of $[45^\circ/-45^\circ/45^\circ]$ laminate from elasticity, present and CST with $S = 5$.

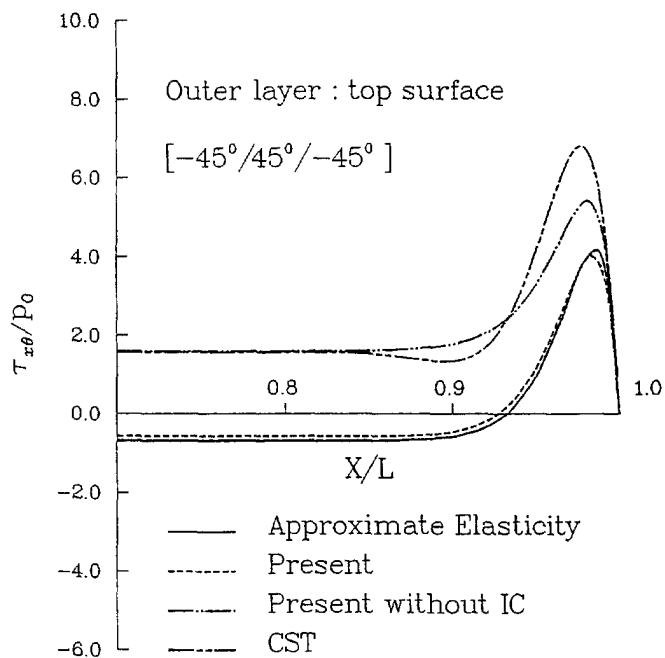


Fig. 15. Comparisons of axial variation of in-plane shear stress of the top surface of $[45^\circ/-45^\circ/45^\circ]$ laminate from elasticity, present and CST with $S = 5$.

from elasticity while almost no improvement in the central region can be found. After the initial curvature effect is also incorporated in the present approach, good comparison with the elasticity solution is found. Thus, it is clear that the reason for CST to have great deviation is the negligence of both effects of shear deformation and initial curvature. Further, the shear deformation is important only in the edge region. Incorporation of the shear effect can only upgrade the results at the edge.

Figure 16 gives the transverse shear stress τ_{xz} along the length of the cylinder from both the elasticity theory and the present approach. It is found that the shear is zero in the

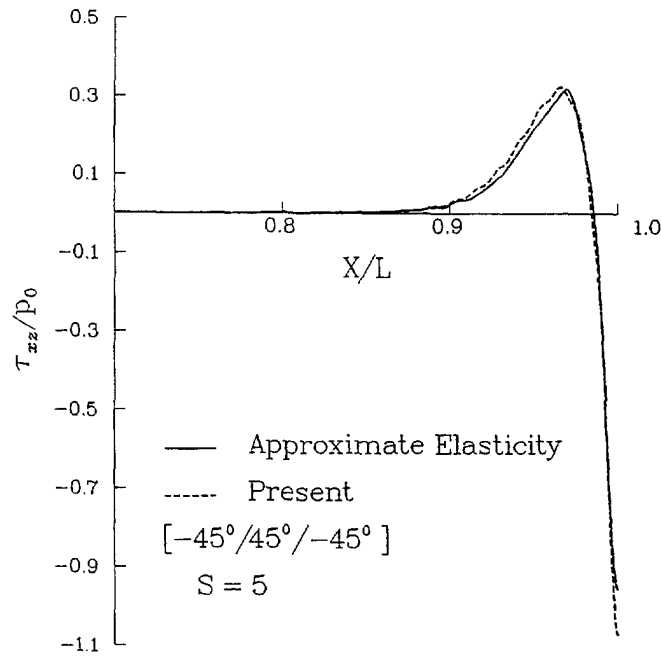


Fig. 16. Comparisons of axial variation of transverse shear stress of the middle surface of $[-45^\circ/45^\circ/45^\circ]$ laminate from elasticity and present with $S = 5$.

central region and has violent changes at the edge. Although the variation in the edge region is quite drastic, the present approach can still satisfactorily predict the stress. The reasonable accuracy of the present theory is thus demonstrated.

CONCLUSIONS

Bending analysis using the mixed shear deformation theory proposed by the authors is extended to arbitrarily laminated anisotropic shell panels and closed cylinders in this study. The effect of shear deformation is considered through the variational approach. Piecewise parabolic distribution is assumed for transverse shear. The initial curvature effect is included in the assumed transverse shear stresses as well as strain-displacement relations and stress resultants. Two examples are studied. Both the cylindrical panels and closed finite cylinder are investigated. From the results shown above, it is quite clear that the present mixed shear deformation theory can satisfactorily predict the behavior of thick shell panels and finite cylinders with arbitrary lamination although only two stacking sequences are studied. Reasonably good results can be found for the displacements, in-plane stresses, transverse shear, and also transverse normal stresses. The main reason is due to the incorporation of effects of shear deformation with mixed formulation and the initial curvature. None of these can be neglected to have a reasonable two-dimensional shell theory.

REFERENCES

- Chaudhuri, R. A. and Abu-Arja, K. R. (1989). Closed-form solutions for arbitrary laminated anisotropic cylindrical shells (tubes) including shear deformation. *AIAA J.* **27**, 1597-1605.
- Chaudhuri, R. A., Bataraman, K. and Kunukkasseril, V. X. (1986). Arbitrarily laminated anisotropic cylindrical shell under internal pressure. *AIAA J.* **24**, 1851-1858.
- Dennis, S. T. and Palazotto, A. N. (1991). Laminated shell in cylindrical bending, two-dimensional approach vs exact. *AIAA J.* **29**, 647-650.
- Di Sciuva, M. (1987). An improved shear-deformation theory for moderately thick multilayered anisotropic shells and plates. *ASME J. Appl. Mech.* **54**, 589-596.
- Dong, S. B. and Tso, F. K. W. (1972). On a laminated orthotropic shell theory including transverse shear deformation. *ASME J. Appl. Mech.* **39**, 1091-1096.

- Hsu, T. M. and Wang, J. T. S. (1970). A theory of laminated cylindrical shells consisting of layers of orthotropic laminae. *AIAA J.* **8**, 2141–2146.
- Jing, H. S. and Liao, M. L. (1989). Partial hybrid stress element for the analysis of thick laminated composite plates. *Int. J. Numer. Meth. Engng* **28**, 2813–2827.
- Jing, H. S. and Tzeng, K. G. (1993a). On two mixed variational principles for thick laminated composite plates. *Compos. Struct.* **23**, 319–337.
- Jing, H. S. and Tzeng, K. G. (1993b). Refined shear deformation theory of laminated shells. *AIAA J.* **31**, 765–773.
- Jing, H. S. and Tzeng, K. G. (1993c). Elasticity solution for laminated anisotropic cylindrical panels in cylindrical bending. To appear in *Compos. Struct.*
- Jing, H. S. and Tzeng, K. G. (1993b). Approximate elasticity solution for arbitrarily laminated anisotropic finite cylinders. *AIAA J.* **31**, 2121–2129.
- Khdeir, A. A., Librescu, L. and Frederick, D. (1989). A shear deformable theory of laminated composite shallow shell-type panels and their response analysis II: static response. *Acta Mech.* **77**, 1–12.
- Murakami, H. (1986). Laminated composite plate theory with improved in-plane responses. *ASME J. Appl. Mech.* **53**, 661–666.
- Reddy, J. N. (1984). Exact solutions of moderately thick laminated shells. *J. Engng Mech.* **110**, 794–809.
- Reddy, J. N. and Liu, C. F. (1985). A higher order shear deformation theory of laminated elastic shells. *Int. J. Engng Sci.* **23**, 319–330.
- Reissner, E. (1984). On a certain mixed variational theorem and a proposed application. *Int. J. Numer. Meth. Engng* **20**, 1366–1368.
- Reissner, E. (1987). On a certain mixed variational theorem and on laminated elasticshell theory. In *Refined Dynamic Theory of Beams, Plates and Shells*, pp. 17–27. Springer-Verlag, Berlin.
- Reuter, R. C. (1972). Analysis of shells under internal pressure. *J. Compos. Mater.* **6**, 94–113.
- Simitses, G. J. and Han, B. (1991). Analysis of anisotropic laminated cylindrical shells subjected to destabilizing loads. Part I: theory and solution procedure. *Compos. Struct.* **19**, 167–181.
- Whitney, J. M. (1971). On the use of shell theory for determinating stress in composite cylinders. *J. Compos. Mater.* **5**, 340–353.
- Whitney, J. M. and Halpin, J. C. (1968). Analysis of laminated anisotropic tubes under combined loadings. *J. Compos. Mater.* **2**, 360–367.

APPENDIX

The matrices $\mathbf{d}_i (i = 1-8), \dots, \mathbf{B}_\beta$ appearing in eqns (3) are given as follows:

$$\begin{aligned} \mathbf{d}_{1_{N \times 1}} &= \left[\left(\frac{e_1}{S_{55} a_1} \right)^{(1)} \cdots \left(\frac{e_1}{S_{55} a_1} \right)^{(N)} \right]^T \\ \mathbf{d}_{2_{N \times 1}} &= \left[\left(\frac{e_1 \lambda_1}{S_{55} a_1} \right)^{(1)} \cdots \left(\frac{e_1 \lambda_1}{S_{55} a_1} \right)^{(N)} \right]^T \\ \mathbf{d}_{3_{N-1 \times 1}} &= [c_1^{(2)} + c_3^{(1)} \cdots c_1^{(N)} + c_3^{(N-1)}]^T \\ \mathbf{d}_{4_{N-1 \times 1}} &= [(c_1 \lambda_1)^{(2)} + (c_3 \lambda_1)^{(1)} \cdots (c_1 \lambda_1)^{(N)} + (c_3 \lambda_1)^{(N-1)}]^T \\ \mathbf{d}_{5_{N \times 1}} &= \left[\left(\frac{e_2}{S_{44} a_2} \right)^{(1)} \cdots \left(\frac{e_2}{S_{44} a_2} \right)^{(N)} \right]^T \\ \mathbf{d}_{6_{N \times 1}} &= \left[\left(\frac{e_2 \lambda_2}{S_{44} a_2} \right)^{(1)} \cdots \left(\frac{e_2 \lambda_2}{S_{44} a_2} \right)^{(N)} \right]^T \\ \mathbf{d}_{7_{N-1 \times 1}} &= [c_2^{(2)} + c_4^{(1)} \cdots c_2^{(N)} + c_4^{(N-1)}]^T \\ \mathbf{d}_{8_{N-1 \times 1}} &= [(c_2 \lambda_2)^{(2)} + (c_4 \lambda_2)^{(1)} \cdots (c_2 \lambda_2)^{(N)} + (c_4 \lambda_2)^{(N-1)}]^T \\ \mathbf{A}_{1_{N \times N-1}} &= \begin{bmatrix} 0 & & \\ (b_1/a_1)^{(k)} & (b_3/a_1)^{(k)} & \\ 0 & & \end{bmatrix} \\ \mathbf{A}_{2_{N \times N-1}} &= \begin{bmatrix} 0 & & \\ (S_{45} b_1/S_{55} a_1)^{(k)} & (S_{45} b_3/S_{55} a_1)^{(k)} & \\ 0 & & \end{bmatrix} \\ \mathbf{A}_{3_{N \times N-1}} &= \begin{bmatrix} 0 & & \\ (S_{45} b_2/S_{44} a_2)^{(k)} & (S_{45} b_4/S_{44} a_2)^{(k)} & \\ 0 & & \end{bmatrix} \end{aligned}$$

$$\begin{aligned}
\mathbf{A}_{4_{N \times N-1}} &= \begin{bmatrix} 0 \\ (b_2/a_2)^{(k)} & (b_4/a_2)^{(k)} \\ 0 \end{bmatrix} \\
\mathbf{B}_{1_{N \times N}} &= \begin{bmatrix} 0 \\ (S_{45}a_3/S_{55}a_1)^{(k)} \\ 0 \end{bmatrix} \\
\mathbf{B}_{2_{N \times N}} &= \begin{bmatrix} 0 \\ (S_{45}a_3/S_{44}a_1)^{(k)} \\ 0 \end{bmatrix} \\
\mathbf{G}_{1_{N-1 \times N-1}} &= \begin{bmatrix} 0 \\ (S_{55}d_2)^{(k)} & [(S_{55}d_3)^{(k)} + (S_{55}d_1)^{(k+1)}] & (S_{55}d_2)^{(k+1)} \\ 0 \end{bmatrix} \\
\mathbf{G}_{2_{N-1 \times N-1}} &= \begin{bmatrix} 0 \\ (S_{45}d_2)^{(k)} & [(S_{45}d_3)^{(k)} + (S_{45}d_1)^{(k+1)}] & (S_{45}d_2)^{(k+1)} \\ 0 \end{bmatrix} \\
\mathbf{G}_{3_{N-1 \times N-1}} &= \begin{bmatrix} 0 \\ (S_{44}d_2)^{(k)} & [(S_{44}d_3)^{(k)} + (S_{44}d_1)^{(k+1)}] & (S_{44}d_2)^{(k+1)} \\ 0 \end{bmatrix} \\
\mathbf{F}_{1_{N-1 \times N}} &= \begin{bmatrix} 0 \\ (S_{55}b_3)^{(k)} & (S_{55}b_1)^{(k+1)} \\ 0 \end{bmatrix} \\
\mathbf{F}_{2_{N-1 \times N}} &= \begin{bmatrix} 0 \\ (S_{45}b_3)^{(k)} & (S_{45}b_1)^{(k+1)} \\ 0 \end{bmatrix} \\
\mathbf{F}_{3_{N-1 \times N}} &= \begin{bmatrix} 0 \\ (S_{44}b_3)^{(k)} & (S_{44}b_1)^{(k+1)} \\ 0 \end{bmatrix}
\end{aligned} \tag{A1}$$

where S_{44} , S_{45} and S_{55} stand for compliance of transverse shear. In the above formulae

$$\lambda_1^{(k)} = (-1)^k 2/h_k, \quad \lambda_2^{(k)} = (-1)^k 2(1 + z_0^{(k)}/R)/h_k$$

and the elements of these matrices are

$$\begin{aligned}
a_1^{(k)} &= \frac{9R^{(k)2}}{4Rh_k^2} (\tilde{g}_0 - 8\tilde{g}_2 + 16\tilde{g}_4) \\
a_2^{(k)} &= \frac{6R^{(k)}}{5Rh_k}; \quad a_3^{(k)} = a_2^{(k)}; \quad b_1^{(k)} = \frac{R^{(k)}}{2R} \\
b_2^{(k)} &= \frac{R^{(k)}}{2R} + \frac{h_k}{20R}; \quad b_3^{(k)} = b_1^{(k)} \\
b_4^{(k)} &= \frac{R^{(k)}}{2R} - \frac{h_k}{20R} \\
c_1^{(k)} &= \frac{h_k^2}{R} \left(\frac{1}{12} + \frac{R^{(k)}}{2h_k} \right); \quad c_2^{(k)} = \frac{h_k}{2} \\
c_3^{(k)} &= \frac{h_k^2}{R} \left(-\frac{1}{12} + \frac{R^{(k)}}{2h_k} \right); \quad c_4^{(k)} = c_2^{(k)} \\
d_1^{(k)} &= \frac{R^{(k)}h_k}{3R} + \frac{h_k^2}{12R}
\end{aligned}$$

$$d_2^{(k)} = \frac{R^{(k)}h_k}{6R}$$

$$d_3^{(k)} = \frac{R^{(k)}h_k}{3R} - \frac{h_k^2}{12R}$$

$$e_1^{(k)} = \frac{R^{(k)}}{R}; \quad e_2^{(k)} = 1$$

where $R^{(k)}$ is the mean radius of the k th layer and

$$\tilde{g}_0 = \sum_{n=1,2,\dots}^{\infty} \frac{\tilde{b}^{-2n+1}}{2^{2(n-1)}(2n-1)}; \quad \tilde{g}_2 = \sum_{n=1,2,\dots}^{\infty} \frac{\tilde{b}^{-2n+1}}{2^{2n}(2n+1)}; \quad \tilde{g}_4 = \sum_{n=1,2,\dots}^{\infty} \frac{\tilde{b}^{-2n+1}}{2^{2(n+1)}(2n+3)}$$

in which $\tilde{b} = R^{(k)}/h_k$. The constants $D_{11}^*, \dots, G_{24}^*$ appearing in eqn (8) are expressed as follows:

$$\begin{aligned} (D_{11}^*, D_{12}^*, D_{13}^*, D_{14}^*) &= \mathcal{L}_1^T(\mathbf{h}_9, \mathbf{h}_{10}, \mathbf{h}_{11}, \mathbf{h}_{12}) + \mathcal{L}_2^T(\mathbf{h}_1, \mathbf{h}_2, \mathbf{h}_3, \mathbf{h}_4) \\ (D_{21}^*, D_{22}^*, D_{23}^*, D_{24}^*) &= \mathcal{L}_3^T(\mathbf{h}_9, \mathbf{h}_{10}, \mathbf{h}_{11}, \mathbf{h}_{12}) + \mathcal{L}_4^T(\mathbf{h}_1, \mathbf{h}_2, \mathbf{h}_3, \mathbf{h}_4) \\ (G_{11}^*, G_{12}^*, G_{13}^*, G_{14}^*) &= \mathbf{m}_1^T(\mathbf{h}_{13}, \mathbf{h}_{14}, \mathbf{h}_{15}, \mathbf{h}_{16}) + \mathbf{m}_2^T(\mathbf{h}_5, \mathbf{h}_6, \mathbf{h}_7, \mathbf{h}_8) \\ (G_{21}^*, G_{22}^*, G_{23}^*, G_{24}^*) &= \mathbf{m}_3^T(\mathbf{h}_{13}, \mathbf{h}_{14}, \mathbf{h}_{15}, \mathbf{h}_{16}) + \mathbf{m}_4^T(\mathbf{h}_5, \mathbf{h}_6, \mathbf{h}_7, \mathbf{h}_8). \end{aligned} \tag{A2}$$

The elements of the above equation are given as

$$\begin{aligned} \mathcal{L}_{1,1 \times N}^T &= [e_1^{(1)} \dots e_1^{(N)}]; \quad \mathcal{L}_{3,1 \times N}^T = [(\lambda_1 e_1)^{(1)} \dots (\lambda_1 e_1)^{(N)}] \\ \mathbf{m}_{1,1 \times N}^T &= [e_2^{(1)} \dots e_2^{(N)}]; \quad \mathbf{m}_{3,1 \times N}^T = [(\lambda_2 e_2)^{(1)} \dots (\lambda_2 e_2)^{(N)}] \\ \mathcal{L}_{2,1 \times N-1}^T &= \mathbf{d}_3^T; \quad \mathcal{L}_{4,1 \times N-1}^T = \mathbf{d}_4^T; \quad \mathbf{m}_{2,1 \times N-1}^T = \mathbf{d}_7^T; \quad \mathbf{m}_{4,1 \times N-1}^T = \mathbf{d}_8^T \\ (\mathbf{h}_1, \mathbf{h}_2, \mathbf{h}_3, \mathbf{h}_4) &= -[\mathbf{a}_1^{-1} \mathbf{a}_2(\mathbf{h}_5, \mathbf{h}_6, \mathbf{h}_7, \mathbf{h}_8) + \mathbf{a}_1^{-1}(\mathbf{b}_1, \mathbf{b}_2, \mathbf{b}_3, \mathbf{b}_4)] \\ (\mathbf{h}_5, \mathbf{h}_6, \mathbf{h}_7, \mathbf{h}_8) &= [\mathbf{a}_4 - \mathbf{a}_3 \mathbf{a}_1^{-1} \mathbf{a}_2]^{-1} [\mathbf{a}_3 \mathbf{a}_1^{-1}(\mathbf{b}_1, \mathbf{b}_2, \mathbf{b}_3, \mathbf{b}_4) - (\mathbf{b}_5, \mathbf{b}_6, \mathbf{b}_7, \mathbf{b}_8)] \\ (\mathbf{h}_9, \mathbf{h}_{10}, \mathbf{h}_{11}, \mathbf{h}_{12}) &= \mathbf{g}_1(\mathbf{h}_1, \mathbf{h}_2, \mathbf{h}_3, \mathbf{h}_4) + \mathbf{g}_2(\mathbf{h}_5, \mathbf{h}_6, \mathbf{h}_7, \mathbf{h}_8) + (\mathbf{g}_3, \mathbf{g}_4, \mathbf{g}_5, \mathbf{g}_6) \\ (\mathbf{h}_{13}, \mathbf{h}_{14}, \mathbf{h}_{15}, \mathbf{h}_{16}) &= \mathbf{f}_1(\mathbf{h}_1, \mathbf{h}_2, \mathbf{h}_3, \mathbf{h}_4) + \mathbf{f}_2(\mathbf{h}_5, \mathbf{h}_6, \mathbf{h}_7, \mathbf{h}_8) + (\mathbf{f}_3, \mathbf{f}_4, \mathbf{f}_5, \mathbf{f}_6) \end{aligned}$$

in which

$$\begin{aligned} (\mathbf{a}_1, \mathbf{a}_2) &= \mathbf{F}_1(\mathbf{g}_1, \mathbf{g}_2) + \mathbf{F}_2(\mathbf{f}_1, \mathbf{f}_2) + (\mathbf{G}_1, \mathbf{G}_2) \\ (\mathbf{a}_3, \mathbf{a}_4) &= \mathbf{F}_3(\mathbf{g}_1, \mathbf{g}_2) + \mathbf{F}_4(\mathbf{f}_1, \mathbf{f}_2) + (\mathbf{G}_2, \mathbf{G}_3) \\ (\mathbf{b}_1, \mathbf{b}_2, \mathbf{b}_3, \mathbf{b}_4) &= \mathbf{F}_1(\mathbf{g}_3, \mathbf{g}_4, \mathbf{g}_5, \mathbf{g}_6) + \mathbf{F}_2(\mathbf{f}_3, \mathbf{f}_4, \mathbf{f}_5, \mathbf{f}_6) - (\mathbf{d}_3, \mathbf{d}_4, 0, 0) \\ (\mathbf{b}_5, \mathbf{b}_6, \mathbf{b}_7, \mathbf{b}_8) &= \mathbf{F}_3(\mathbf{g}_3, \mathbf{g}_4, \mathbf{g}_5, \mathbf{g}_6) + \mathbf{F}_4(\mathbf{f}_3, \mathbf{f}_4, \mathbf{f}_5, \mathbf{f}_6) - (\mathbf{d}_7, \mathbf{d}_8, 0, 0). \end{aligned}$$

The matrices $\mathbf{f}_1, \dots, \mathbf{g}_6$ in the above formulae are

$$\begin{aligned} (\mathbf{f}_1, \mathbf{f}_2, \mathbf{f}_3, \mathbf{f}_4, \mathbf{f}_5, \mathbf{f}_6) &= [\mathbf{I} - \mathbf{B}_2 \mathbf{B}_1]^{-1} [\mathbf{B}_2(\mathbf{A}_1, \mathbf{A}_2, -\mathbf{d}_1, -\mathbf{d}_2, 0, 0) + (-\mathbf{A}_3, -\mathbf{A}_4, 0, 0, \mathbf{d}_5, \mathbf{d}_6)] \\ (\mathbf{g}_1, \mathbf{g}_2, \mathbf{g}_3, \mathbf{g}_4, \mathbf{g}_5, \mathbf{g}_6) &= (-\mathbf{A}_1, -\mathbf{A}_2, \mathbf{d}_1, \mathbf{d}_2, 0, 0) - \mathbf{B}_1(\mathbf{f}_1, \mathbf{f}_2, \mathbf{f}_3, \mathbf{f}_4, \mathbf{f}_5, \mathbf{f}_6) \end{aligned}$$

where \mathbf{I} is an $N \times N$ identity matrix and the superscript -1 stands for the inverse of a matrix.